

EFFICIENT EXPERIMENTAL VALIDATION OF STOCHASTIC SENSITIVITY ANALYSES OF SMART SYSTEMS

Steffen Ochs, Sushan Li, Christian Adams, Tobias Melz

research group System Reliability and Machine Acoustics SzM, TU Darmstadt
Magdalenenstraße 4, 64289 Darmstadt, Germany

ochs@szm.tu-darmstadt.de
sLi@szm.tu-darmstadt.de
adams@szm.tu-darmstadt.de
melz@szm.tu-darmstadt.de

Key words: Stochastic simulation, Sensitivity analyses, Experimental validation, Model-based experimental design, Piezoelectric elements, Smart (beam) system

Summary: *A method for the efficient experimental validation of stochastic sensitivity analyses is proposed and tested using a smart system for vibration reduction. Stochastic analyses are needed to assess the reliability and robustness of smart systems. A model-based design of experiments allows the alignment of an experimental design with the results of a previous numerical sensitivity analysis. An exemplary system of structural dynamics is used to test the method. The case of active suppression of disturbing vibrations of a cantilever beam through active piezoelectric elements is considered. The observed target variables are the level of vibration reduction at the beam's end and the location of the fundamental frequency under five uncertain system variables. Based on a numerical model of the piezoelectric beam a variance-based sensitivity analysis is performed to determine each variable's impact on the target variables. Ensuing from these numerical results, a model-based experimental design is established and the experiments are conducted. In comparison to a fully five-factor factorial experimental design the model-based approach reduced the experimental effort by 50%, without great loss of information.*

1 INTRODUCTION

Looking for new promising approaches for solving technical problems, e.g., in the field of vibration reduction, the development of smart systems is becoming more prominent. A smart structure system is characterized by a structure-compliant integration of actuators and sensors on the basis of multi-functional materials such as piezoceramics. The resulting interactions between structural components, sensors, actuators, and control hinder the analysis of the system reliability. In order to factor in such interactions, statistical variation of the system variables needs to be considered in a numerical simulation. In Chapter 2, the proceedings of a variance-based sensitivity analysis are presented and performed on a smart beam structure. Variance-based sensitivity analyses serve as an example for such a numerical simulation.

In Chapter 3 a method for the experimental validation of the numerical results is presented. The methods of Design of Experiments (DoE) [1] can be used. But a quantitative experimental validation of the numerical results is difficult due to the random-based selection of simulation combinations in the stochastic analysis. Only a small amount of simulation combinations can be checked experimentally. Thus, the interactions also need to be confirmed with only a few simulation combinations. In contrast to the non-optimal experimental design, the model-based experimental design can be adapted to an expected model equation. The model-based experimental design allows an alignment of the study on the system behavior under investigation and, thus, offers the possibility of an efficient validation of the numerical results.

2 VARIANCE-BASED SENSITIVITY ANALYSIS OF A PIEZOELECTRIC BEAM

2.1 Stochastic Sensitivity Analysis

Diverse methods to explore the relationship between the input and output variables of a system are summarized under the term sensitivity analysis. It is generally differentiated between local and global techniques [2]. An essential feature of local sensitivity techniques is the observation of localized output variables of a system resulting from small changes in the input variables. The major disadvantage of these techniques lies in the sectionally limited insight and the associated lack of ability to identify interactions. Global methods of sensitivity analysis, however, assume no limitations of the considered area for the design variables. The sensitivity is quantified using the total values of the variables space. A corresponding approach relies on an analysis of variance for the observed output as a basis for assessing the sensitivity [3]. Where the scattering behavior of each design variable is determined by assigning a density function. The respective influence of the design variable X_i is calculated on the scattering behavior of the system and expressed by two sensitivity indices. The direct impact of a design variable X_i is expressed through the main effect

$$S_{M_i} = \frac{\text{Var}[E(Y|X_i)]}{\text{Var}[Y]}, \quad (1)$$

where the variance generated by X_i , represented by the variance of the conditional expected value $\text{Var}[E(Y|X_i)]$, is based on the total variance of the observed output variable $\text{Var}[Y]$.

The total effect

$$S_{T_i} = 1 - \frac{\text{Var}[E(Y|\mathbf{X}_{-i})]}{\text{Var}[Y]} \quad (2)$$

indicates the total influence of a design variable on the observed output and summarizes all effects of X_i , where \mathbf{X}_{-i} represents all influencing design variables without X_i . Variations that arise due to interactions are represented by the difference between the total and the main effect.

The main effect of a variable can reach a value between 0 (no direct relationship) and 1 (strong direct relationship). The total effect can be equal to or greater than the main effect. Equality between the main and the total effect of X_i indicate no interactions with \mathbf{X}_{-i} .

For the considered smart system, both sensitivity indices are determined using a Monte Carlo simulation. The statistical estimators of Sobol' [4] and Jansen [5] are used to calculate the indices from the results of the Monte Carlo simulation.

2.2 Mathematical Model of Piezoelectric Beam Dynamics

The investigated system is a cantilever beam with a flat collocated piezoelectric sensor (S) and actuator (A) pair, as shown in Figure 1. Its properties are summarized in Table 1.

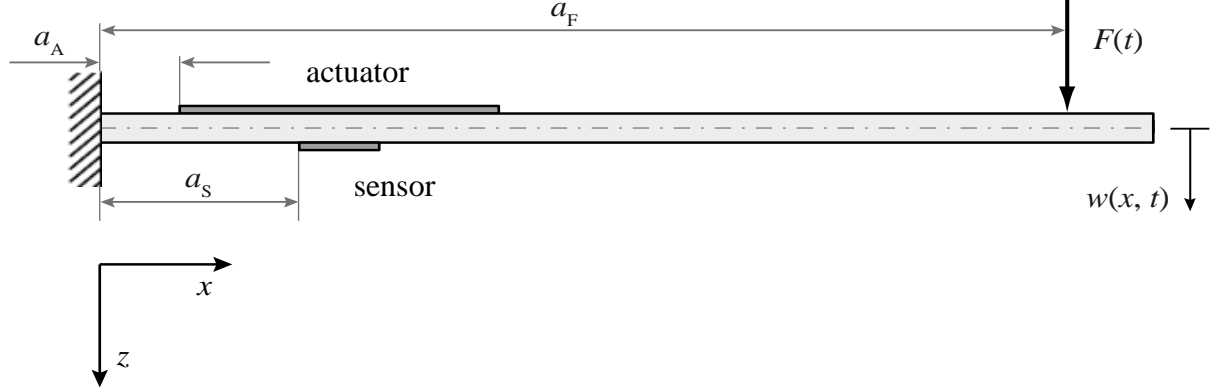


Figure 1: Piezoelectric beam.

The clamped beam is modeled as a EULER-BERNOULLI beam with a lateral load $F(t)$ close to the free end of the beam. A mathematical model governing the motion of the piezoelectric cantilevered beam can be derived by using Hamilton's principle and the assumed mode method [6, 7]. Only the eigenvalue problem of lateral vibration in z -direction $w(x, t)$ is presented in this paper. The lateral displacement in z -direction

$$w(x, t) = \mathbf{\Phi}(x)\mathbf{q}(t) = \sum_{i=1}^n \Phi_i(x)q_i(t) \quad (3)$$

is separated into the spatial solution $\mathbf{\Phi}(x)$ and the temporal solution $\mathbf{q}(t)$. The overall spatial solution is given by

$$\Phi_i(x) = \sinh(\beta_i x) - \sin(\beta_i x) - \frac{\sinh(\beta_i l_B) + \sin(\beta_i l_B)}{\cosh(\beta_i l_B) + \cos(\beta_i l_B)} (\cosh(\beta_i x) - \cos(\beta_i x)). \quad (4)$$

The values for the product $\beta_i l_B$ emerge from the zero crossings of the characteristic equation of a cantilever beam. For the first three eigenmodes they amount to $\beta_1 l_B = 1.8751$; $\beta_2 l_B = 4.6941$; $\beta_3 l_B = 7.8548$. The model is obtained by modal truncation taking only the beam's first three modes of vibration into account. The second-order modal equation in z -direction is given by

$$\begin{aligned} & \left(\rho_B h_B b_B \int_0^{l_B} \Phi_i^2(x) dx + \rho_A h_A b_A \int_0^{l_B} \Phi_i^2(x) H_A dx + \rho_S h_S b_S \int_0^{l_B} \Phi_i^2(x) H_S dx \right) \cdot \ddot{q}_i(t) \dots \\ & + \left(E_B I_B \int_0^{l_B} \Phi_i''^2(x) dx + E_A I_A \int_0^{l_B} \Phi_i''^2(x) H_A dx + E_S I_S \int_0^{l_B} \Phi_i''^2(x) H_S dx \right) \cdot q_i(t) \\ & = \Phi_i(x_F) F(t) - \frac{1}{2} (h_B + h_A) b_A E_A d_{31,A} V_A(t) \int_0^{l_B} \Phi_i(x) H_A'' dx, \end{aligned} \quad (5)$$

where $V_A(t)$ is the voltage applied to the piezoelectric actuator.

Since the actuator and sensor are not attached over the entire length of the beam, their positions need to be considered by means of Heaviside functions

$$H_A = H(x - a_A) - H(x - a_A - l_A) \quad (6)$$

and

$$H_S = H(x - a_S) - H(x - a_S - l_S). \quad (7)$$

The structural damping of the model is defined according to the Rayleigh damping, which is a mass- and stiffness-proportional damping. The coefficients of the Rayleigh damping correspond to a damping ratio of 1.5%, which was analyzed in experimental studies. Finally, the second-order modal equation is converted into a first-order state-space form to link the model with a controller.

symbol	description	value	unit
l_B	length of beam	200	mm
h_B	thickness of beam	3	mm
b_B	width of beam	40	mm
ρ_B	density of beam	2700	kg/m ³
E_B	Young's modulus of beam	70	GPA
I_B	moment of inertia of beam	90	mm ⁴
l_A	length of piezoelectric actuator	50	mm
h_A	thickness of piezoelectric actuator	0.8	mm
b_A	width of piezoelectric actuator	30	mm
a_A	position of piezoelectric actuator	15	mm
ρ_A	density of piezoelectric actuator	7800	kg/m ³
E_A	Young's modulus of piezoelectric actuator	62.1	GPA
I_A	moment of inertia of piezoelectric actuator	1.28	mm ⁴
$d_{31,A}$	piezoelectric constant of actuator	$-1.8 \cdot 10^{-10}$	m/V
l_S	length of piezoelectric sensor	10	mm
h_S	thickness of piezoelectric sensor	0.5	mm
b_S	width of piezoelectric sensor	10	mm
a_S	position of piezoelectric sensor	35	mm
ρ_S	density of piezoelectric sensor	7800	kg/m ³
E_S	Young's modulus of piezoelectric sensor	66.7	GPA
I_S	moment of inertia of piezoelectric sensor	0.104	mm ⁴
$d_{31,S}$	piezoelectric constant of sensor	$-2.1 \cdot 10^{-10}$	m/V
a_F	position of lateral load	$0.95 \cdot l_B$	mm
ζ	structural damping ratio	1.5	%

Table 1: Characteristic data of the piezoelectric beam.

2.3 Control Design

The vibration suppression method Positive Position Feedback (PPF) is implemented to control the vibrations of the beam. PPF control was introduced by Goh and Caughey [8]. It consists of a second-order compensator; thus, it is not sensitive to spillover. Based on the fact that the position-proportional measurement is positively fed into the compensator and the signal from the compensator, magnified by a gain, is positively fed back to the structure the term ‘positive position’ is defined. This property makes the PPF controller very suitable for collocated actuators and sensors.

The advantage of the PPF controller is that the damping of a specific frequency band can be increased. However, one PPF controller can suppress only one mode at a time. Hence, only the vibration suppression of the beam’s first mode (fundamental frequency) is presented in this paper. The charge generated in the piezoelectric sensor due to the deformation is calculated according to Preumont [9]

$$Q_S(t) = \frac{E_S d_{31,S} (h_B + h_S) b_S}{2} (w'(x = a_S + l_S, t) - w'(x = a_S, t)). \quad (8)$$

A charge amplifier, which is connected to the piezoelectric sensor, converts the charge at the input of the amplifier to a voltage at the output. The sensor’s voltage

$$V_S(t) = \frac{Q_S(t)}{C_f} \quad (9)$$

is the input of the PPF controller and $V_A(t)$ is the calculated output. Here, C_f represents the capacitance of the charge amplifier. The transfer function in the Laplace domain that describes the operation of the PPF compensator is

$$C(s) = \frac{g_c \omega_c^2}{s^2 + 2\zeta_c \omega_c s + \omega_c^2}, \quad (10)$$

where ω_c is the compensator’s circular frequency, ζ_c is the compensator damping coefficient, and g_c is the feedback gain coefficient. All properties of the compensator and the charge amplifier are summarized in Table 2.

symbol	description	value	unit
ω_c	compensator circular frequency	$2\pi \cdot 60$	1/s
ζ_c	compensator damping coefficient	0.5	-
g_c	feedback gain coefficient	0.9	s^2
C_f	capacity of charge amplifier	1	nF

Table 2: Characteristic data of the PPF compensator and the charge amplifier.

2.4 Numerical Results of a Monte Carlo Simulation

Five design variables are selected for the stochastic analysis: the length of the beam l_B , the positions of the piezoelectric elements a_A and a_S , the position of the lateral load a_F , and the feedback gain coefficient g_c . The scattering behavior of the design variables is characterized by specified density functions; therefore, uniform distributions between upper and lower limits are chosen. These limits are summarized in Table 3.

symbol	description	lower limit	upper limit	unit
$X_1 = l_B$	length of beam	195	205	mm
$X_2 = a_A$	position of piezoelectric actuator	7	23	mm
$X_3 = a_S$	position of piezoelectric sensor	27	43	mm
$X_4 = a_F$	position of lateral load	$0.85 \cdot l_B$	$0.95 \cdot l_B$	mm
$X_5 = g_c$	feedback gain coefficient	0.8	0.9	s^2

Table 3: Lower and upper limits of the uniform distributions.

It is expected that the variables X_1 , X_2 , X_3 , and X_5 have a direct impact on the system behavior because they affect the action of the PPF controller. The position of the force X_4 has no importance for the control of the fundamental frequency; therefore, no influence should be determined from the Monte Carlo simulation. Furthermore, the Monte Carlo simulation should show whether interactions between the design variables affect the system behavior.

Figure 2 exemplifies the transfer function between velocity and load of the free beam end for the passive system without PPF control and the active system with PPF control.

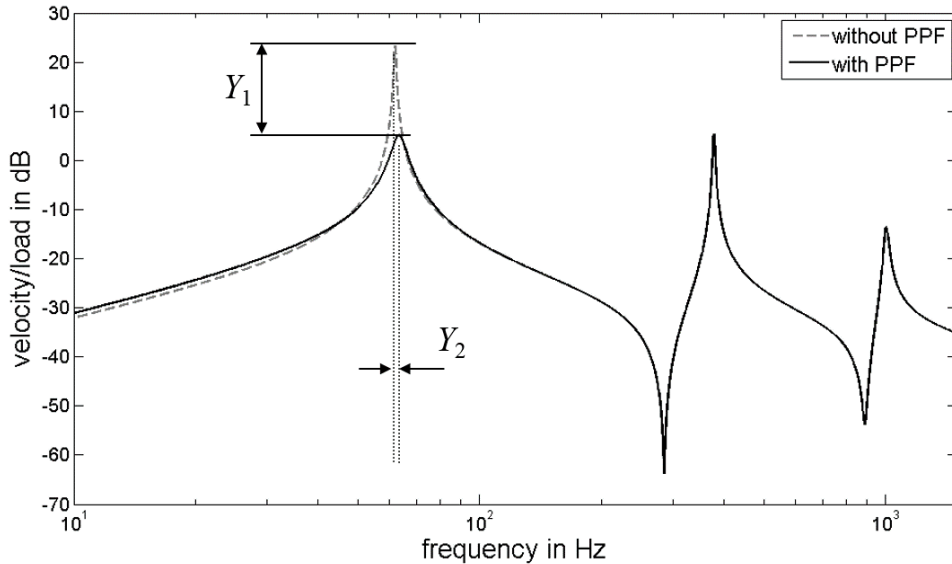


Figure 2: Schematic diagram of the transfer function between velocity and load of the free end of the beam.

The implemented single mode PPF controller produces a significant reduction of vibration at the tuned mode. The other modes are not affected. The level of resonance amplitude reduction Y_1 and the offset of the fundamental frequency Y_2 are considered as output variables of the system.

The sensitivity analysis is performed using the method presented in Section 2.1. The sample for the corresponding Monte Carlo simulation is created with Sobol' sequences with a sample size of $N = 20000$. The calculated main and total effects to the outputs Y_1 and Y_2 are shown in Figure 3. The individual columns stand for the respective main and total effect of a design variable per output. The sum of all main effects of an output is 1.

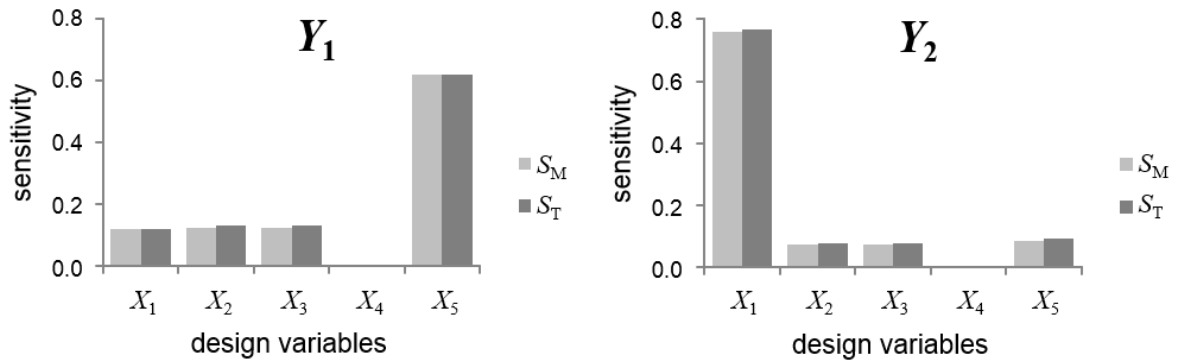


Figure 3: Calculated main and total effects of the design variables to the outputs.

The feedback gain coefficient X_5 has the highest impact on the amplitude reduction Y_1 . Moreover, the positions of the piezoelectric elements X_2 and X_3 have an influence, but not in the same order as the gain coefficient. As expected, the influence of the position of the lateral load X_4 is very low, because it does not affect the quality of the PPF control.

The analysis of the first resonance frequency offset Y_2 shows a different behavior. The length of the beam X_1 has the highest impact. The influence of the other variables is very low. The numerical analysis also demonstrates that no strong interactions appear in both output variables. The correctness of these results will now be confirmed by an experimental validation. The required approach is described in the next chapter.

3 EXPERIMENTAL VALIDATION OF STOCHASTIC SENSITIVITY ANALYSES

3.1 Model-based Experimental Design

In principle, the methods of DoE [1] are suitable for the experimental validation of the numerical sensitivity analysis, because interactions can be detected with most designs. According to the classical approach of DoE either factorial or fractional factorial (non-optimal) designs can be used. Furthermore, a model-based design of experiments, also called optimal design, allows the alignment of an experimental design with the results of a previous numerical sensitivity analysis. Thus, the number of necessary experiments can be reduced, compared to the non-optimal design. Various statistical criteria are available to optimize the experimental design. In this work, the D-optimality criterion is used [10], which seeks to maximize the determinant of the information matrix $\mathbf{X}^T\mathbf{X}$ of the design where \mathbf{X} is the matrix of the design variables. A D-optimal design is not generated with a fixed pattern, but constructed iteratively so that the determinant of the information matrix is maximized. This process is carried out with a coordinate exchange algorithm [11].

Under the assumption of a linear system behavior (theory of EULER-BERNOULLI) the consideration of two levels per variable is acceptable. The upper and lower limits of the numerical analysis (Table 3) denoted with (+) and (-) are used for these two levels. A five-factor factorial experimental design with $2^5 = 32$ simulation combinations would be necessary. But the results of the numerical analysis in Section 2.4 shows that no strong interactions appear in both outputs. Hence, interactions of higher order do not need to be considered.

The use of a D-optimal experimental design would require only 16 simulation combinations (SC) as listed in Table 4. With this design, the second-order interactions can be analyzed to confirm the results of the numerical analysis. Higher order interactions are not considered because they are not probable. In contrast to a five-factor factorial experimental design the model-based approach reduced the experimental effort by 50%, without great loss of information.

SC	X_1	X_2	X_3	X_4	X_5	SC	X_1	X_2	X_3	X_4	X_5
1	(-)	(-)	(+)	(-)	(-)	9	(+)	(-)	(-)	(-)	(-)
2	(-)	(+)	(-)	(-)	(-)	10	(+)	(+)	(+)	(-)	(-)
3	(-)	(-)	(-)	(-)	(+)	11	(+)	(-)	(+)	(-)	(+)
4	(-)	(+)	(+)	(-)	(+)	12	(+)	(+)	(-)	(-)	(+)
5	(-)	(-)	(-)	(+)	(-)	13	(+)	(-)	(+)	(+)	(-)
6	(-)	(+)	(+)	(+)	(-)	14	(+)	(+)	(-)	(+)	(-)
7	(-)	(-)	(+)	(+)	(+)	15	(+)	(-)	(-)	(+)	(+)
8	(-)	(+)	(-)	(+)	(+)	16	(+)	(+)	(+)	(+)	(+)

Table 4: Simulation combinations (SC) of the optimal experimental design.

3.2 Experimental Setup

A test bench is set up to check the usability of the optimal experimental design for the validation of numerical sensitivity indices. It is shown in Figure 4.

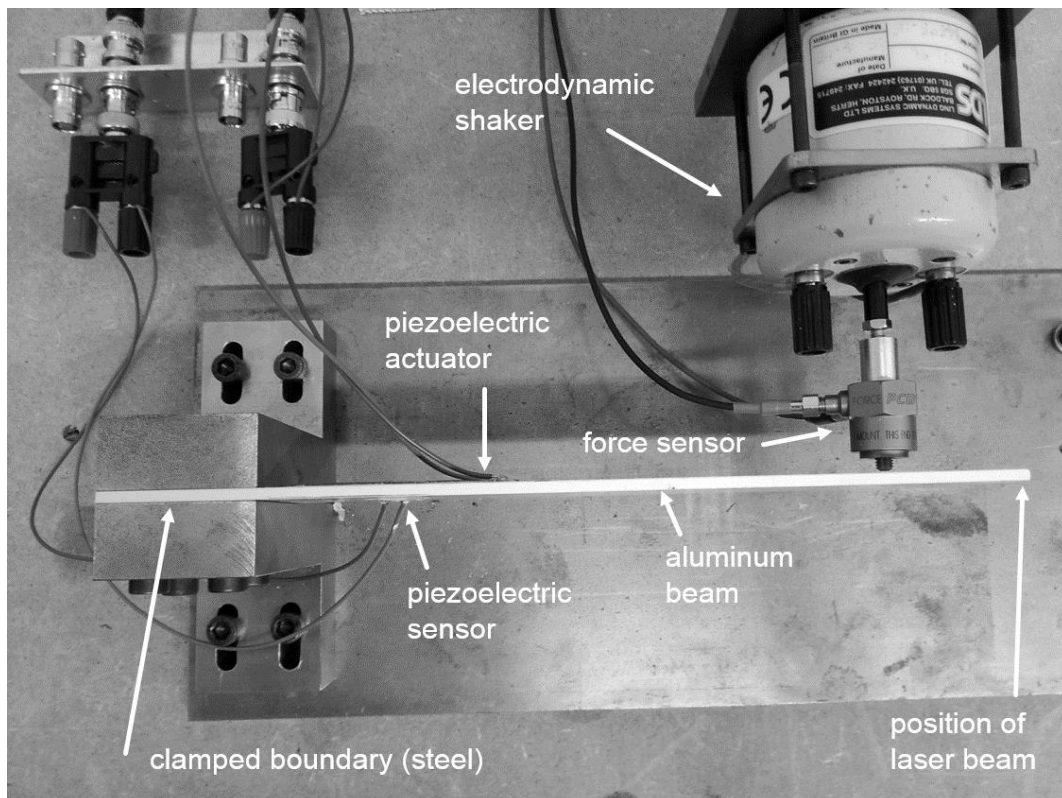


Figure 4: Experimental configuration (view from top).

Various beams consisting of aluminum and piezoelectric elements are fabricated for the experimental studies, such as those described in the experimental design (Tables 3 and 4). The used piezoelectric materials are PIC151 for the sensor and PIC255 for the actuator. The piezoelectric materials are bonded to the beam with an adhesive film. The beam is clamped with two thick steel brackets bolted to a heavy block of steel. Real-time active vibration suppression is implemented using a dSPACE digital control system. The block diagram of the PPF control system, built in Simulink, is converted to C-code, which is then compiled and implemented on the dSPACE hardware to achieve real-time simulation and control. The lateral load is simulated by a force impulse with an electrodynamic shaker. The impact is recorded with a force sensor and the velocity is measured with a laser vibrometer, whose laser beam is directed to the end of the piezoelectric beam.

3.3 Experimental Validation

In this section, numerical (n) and experimental (e) response functions for the passive system without PPF control and the active system with PPF control are compared, followed by an experimental validation of the numerical sensitivity indices.

The challenge in the experimental validation of numerical results lies in ensuring identical boundary conditions. A stiff connection of the electrodynamic shaker to the beam would affect the system behavior of the piezoelectric beam. Therefore, the beam system is excited by a force impulse. The response of the smart beam (SC 16) to a force impulse of 3 N at 0.1 s is shown in Figure 5. The numerically calculated system response is illustrated in the left diagram. The decay time of the active system is reduced by 85%, compared to the uncontrolled system, due to the damping introduced by the PPF controller. The numerically calculated system behavior is consistent with the real system behavior, as shown in the left diagram of Figure 5.

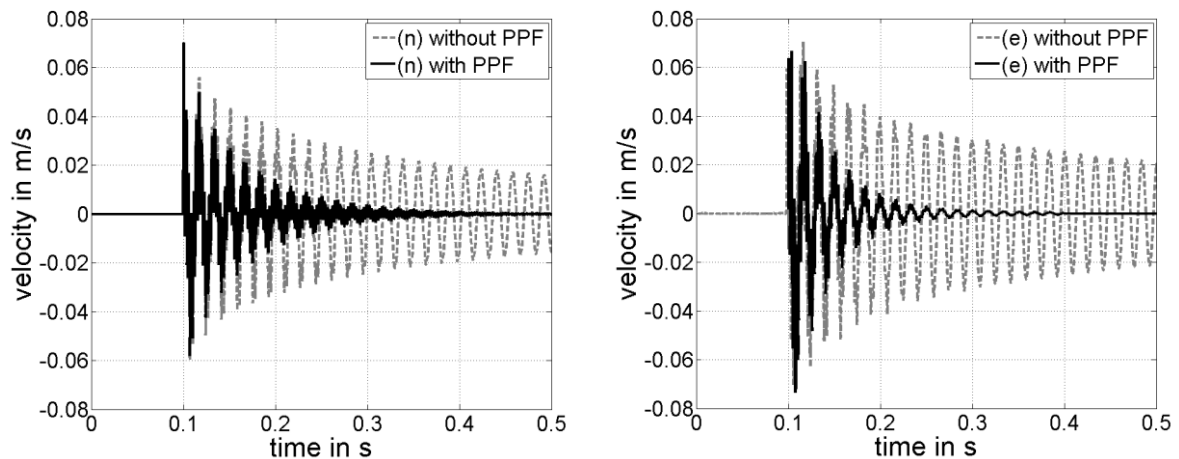


Figure 5: Impulse response function (SC 16), with a load $F = 3$ N, calculated numerically (n) on the left, measured experimentally (e) on the right.

There is also excellent agreement between the experimental and the numerical values for the fundamental frequency as shown in Figure 6.

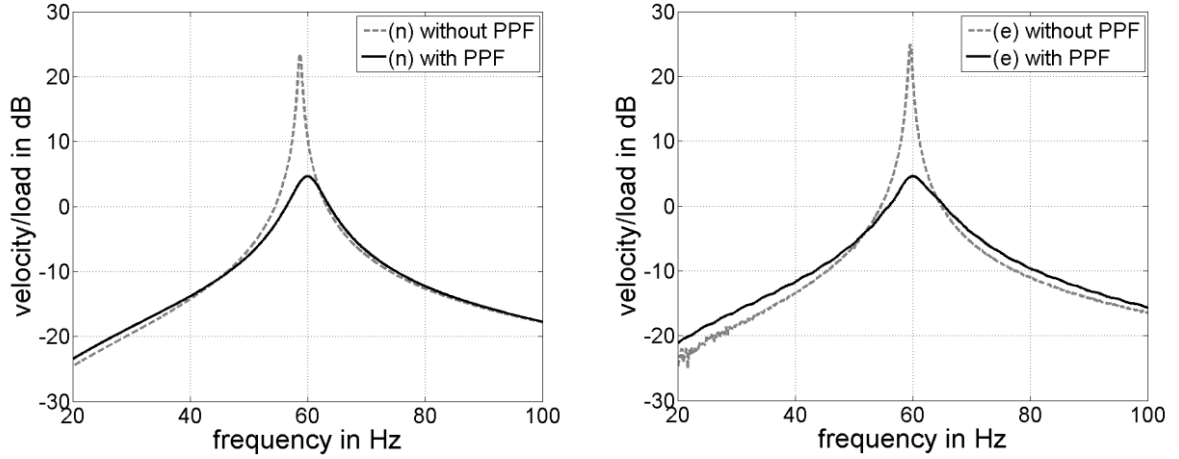


Figure 6: Impulse transfer function between velocity and load of a beam with the simulation combination SC16, calculated numerically (n) on the left, measured experimentally (e) on the right.

The experimental sensitivity indices are not calculated like the numerical indices in Section 2.1. The number of simulation combinations is insufficient. In a two-level factorial design the effect

$$E_{X_i} = \bar{Y}_{X_i^+} - \bar{Y}_{X_i^-} \quad (11)$$

of a variable X_i is defined as the change in response Y produced by a change in the level of that variable averaged over the levels of the other variables. Thus, the effect of X_1 is calculated as the average of the results of SC 9–16 less the average of the results of SC 1–8. The effect index

$$\hat{E}_{X_i} = \frac{|E_{X_i}|}{\sum_{i=1}^5 |E_{X_i}|} \quad (12)$$

is based on the sum of all absolute effects for comparison with the calculated main effect S_M of the numerical simulation. All calculated sensitivity indices S_{M_i} and \hat{E}_{X_i} of the design variables to the outputs Y_1 and Y_2 are shown in Figure 7.

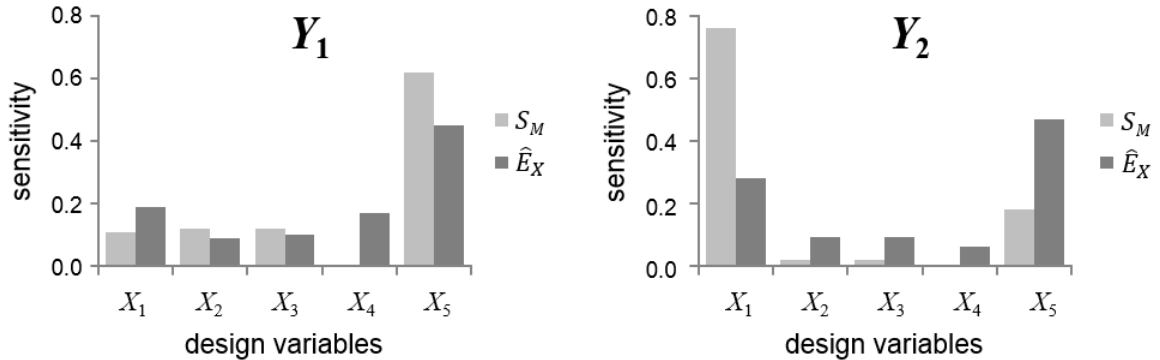


Figure 7: Comparison of the calculated main effects of the design variables to the outputs.

For output Y_1 the calculated indices closely match. In the experiment, however, an influence of the position of the load X_4 is demonstrated, which was not recognized in the numerical simulation. This influence can also be seen in the results for output Y_2 . The large influence of the length of the beam X_1 on the amplitude reduction Y_2 cannot be confirmed in the experiment.

Instead, a much larger impact of the feedback gain coefficient X_5 is identified.

In Section 2.4 the results of the numerical analysis shows that no strong interactions appear in both outputs. To verify this results, the effects of interactions X_{ij} can be calculated similarly to Equation (11) from the experimental data. The results for Y_1 are shown in Figure 8.

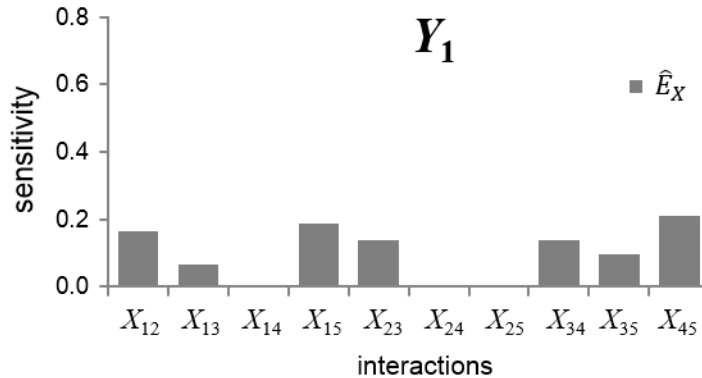


Figure 8: 2nd order interaction effects to the output Y_1 .

Expectedly, interaction effects can be seen. The comparison with Figure 7 shows that some interactions have a similar magnitude to the design variables; thus, they cannot be ignored. In a further experiment it will be analyzed whether in addition to the second-order interactions even higher order interactions exist. For this a full factorial design will be incorporated. It will only be necessary to test 16 additional simulation combinations, as the results of the optimal design can be reused.

4 CONCLUSIONS

A method for the efficient experimental validation of stochastic sensitivity analyses is proposed and tested using a smart system for vibration reduction. It is shown that the methods of DoE are suitable for the experimental validation of numerical sensitivity indices. A quantitative experimental validation of the numerical results is difficult due to the random-based selection of simulation combinations in the stochastic analysis. Only a small amount of simulation combinations can be checked experimentally. A model-based design of experiments, also called optimal design, allows the alignment of an experimental design with the results of the previous numerical sensitivity analysis. Thus, the number of necessary experiments can be reduced, compared to the non-optimal design.

REFERENCES

- [1] D. Montgomery, *Design and Analysis of Experiments*. John Wiley & Sons, Chichester, 2006.
- [2] A. Saltelli et al., *Sensitivity Analysis in Practice*. John Wiley & Sons, Chichester, 2004.
- [3] A. Saltelli et al., *Global Sensitivity Analysis – The Primer*. John Wiley & Sons, Chichester, 2008.

- [4] I.M. Sobol', Sensitivity Estimates for Nonlinear Mathematical Models. *Mathematical Modeling and Computational Experiment*, **1**, 407–414, 1993.
- [5] M.J.W. Jansen, Analysis of variance designs for model output. *Computer Physics Communications*, **117**, 35–43, 1999.
- [6] S. Hong et al., Vibration control of beams using multiobjective state-feedback control. *Smart Materials and Structures*, **15**, 157–163, 2006.
- [7] C.H. Park, Dynamics modelling of beams with shunted piezoelectric elements. *Journal of Sound and Vibration*, **268**, 115–129, 2003.
- [8] C.J. Goh and T.K. Caughey, On the stability problem caused by finite actuator dynamics in the collocated control of large space structures. *International Journal of Control*, **41**, 787–802, 1985.
- [9] A. Preumont, *Vibration Control of Active Structures - An Introduction*, Kluwer Academic Publishers, 2002.
- [10] E. Walter and L. Pronzato, Robust Experiment Design via Stochastic Approximation. *Mathematical Biosciences*, **75**, 103–120, 1985.
- [11] R.K. Meyer and C.J. Nachtsheim, The Coordinate-Exchange Algorithm for Constructing Exact Optimal Experimental Designs. *Technometrics*, **37**, 60–69, 1995.